

The sensitivity of ECE simulations in MAST to different magnetic equilibria models

J. Preinhaelter¹⁾, V. Shevchenko²⁾, M. Valovic²⁾, H. Wilson²⁾, J. Urban¹⁾,
P. Pavlo¹⁾, L. Vahala³⁾, G. Vahala⁴⁾, and the MAST team²⁾

- 1) EURATOM/IPP.CR Association, Institute of Plasma Physics, 182 21 Prague, Czech Republic
 2) EURATOM/UKAEA Fusion Association, Culham Science Centre, Abingdon, OX14 3DB, UK
 3) Old Dominion University, Norfolk, VA 23529, USA
 4) College of William & Mary, Williamsburg, VA 23185, USA

Abstract. ECE simulation based on EFIT and SCENE magnetic equilibria in MAST is compared with detected signal. Nice fit is found for the L-modes and ELMy H-mode where both models give the same results. ECE from ELM-free H-mode has rather intricate structure and our models do not fit well with experiment. Simulations based on EFIT predict proper number of ECE bands but their position is better estimated by SCENE, which takes into account the edge currents.

Introduction. Extensive ECE data from 16 to 60 GHz are available in MAST [1]. The characteristic low magnetic field and high plasma density of a spherical tokamak do not permit the typical radiation of O and X modes from the first five electron cyclotron harmonics. Thus only electron Bernstein modes (modes not subject to a density limit), which mode convert into electromagnetic waves in the upper hybrid resonance region, can be responsible for the measured radiation [2].

3D plasma and antenna model. The instantaneous magnetic field and its spatial derivatives are reconstructed from 2D splining of two potentials determined by equilibrium reconstruction codes (EFIT or SCENE), assuming toroidal symmetry. Plasma density and temperature profiles in the whole RZ cross-section of the plasma are obtained from mapping of the high spatial resolution Thomson scattering measurements onto magnetic surfaces. We improved our 3D plasma model [4] by inclusion of the complete ECE antenna geometry (see Fig. 1). We use the Gaussian beam formalism to find waist positions (one in the horn and the second in front of the window) between mirrors. Only linearly polarized waves are detected by our radiometer and the plane of polarization can be selected by the orientation of the polarization rotator.

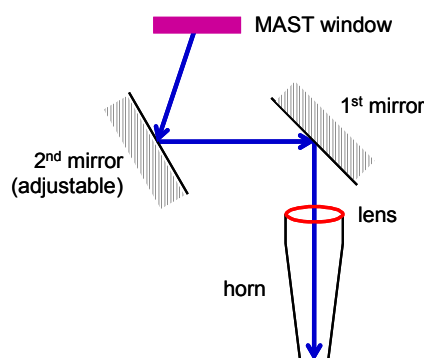


Fig 1. ECE antenna on MAST. Ray between the second mirror and the window is inclined at φ_{dev} from the equatorial plane upward and the angle between its projection onto the equatorial plane and the vertical plane going through the tokamak axis and the antenna position is φ_{long} .

lected by the orientation of the polarization rotator.

To simplify the computation we use a separate set of straight rays to project the rim of window and the visible area onto the second waist plane. Such an approach takes into account the shape of the Gaussian beam in the near and far antenna regions. At the intersection of the rays with the last closed flux surface ('spots') we consider an auxiliary

the instantaneous magnetic field and its spatial derivatives are reconstructed from 2D splining of two potentials determined by equilibrium reconstruction codes (EFIT or SCENE), assuming toroidal symmetry. Plasma density and temperature profiles in the whole RZ cross-section of the plasma are obtained from mapping of the high spatial resolution Thomson scattering measurements onto magnetic surfaces. We improved our 3D plasma model [4] by inclusion of the complete ECE antenna geometry (see Fig. 1). We use the Gaussian beam formalism to find waist positions (one in the horn and the second in front of the window) between mirrors. Only linearly polarized waves are detected by our radiometer and the plane of polarization can be selected by the orientation of the polarization rotator.

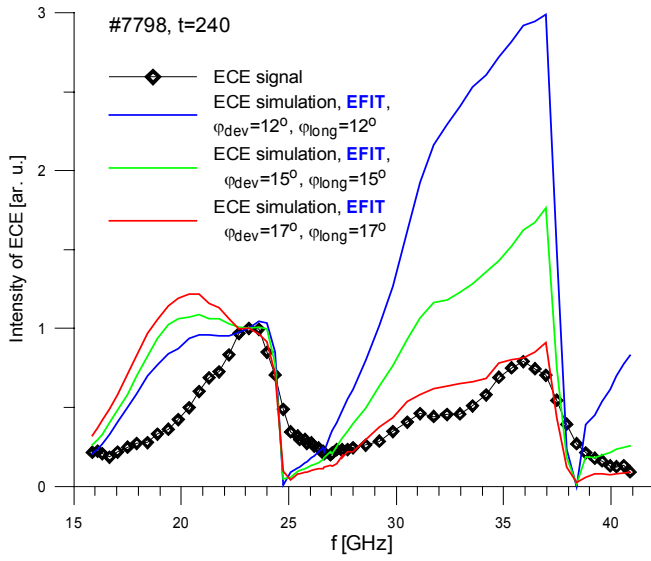


Fig. 2. Effect of several antenna beam aiming on the fit between ECE simulation (EFIT) and detected signal.

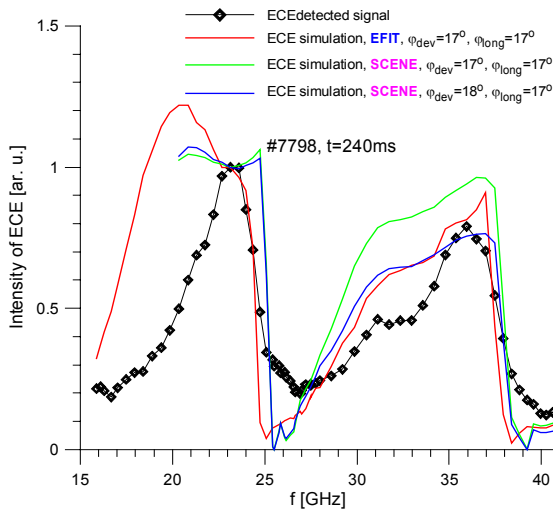


Fig. 3 Comparison of ECE simulation for EFIT and SCENE equilibria for L-mode, #7798.

ray evolution equation. This approach takes into account the reabsorption of radiation, which is important for non-local wave damping.

Simulated ECE power detected by antenna. The intensity of ECE detected by the antenna can be expressed as

$$I_{ECE} = const \times \iint dS W_{Gauss} C_{EBW-X-O} \omega^2 T_{rad} C_{window} V_{relat}$$

where the Gaussian weight $W_{Gauss} = e^{-(2r^2/w_0^2)}$, w_0 is the beam waist radius, $C_{EBW-X-O}$ is the mode conversion efficiency, $\omega^2 T_{rad}$ is the Rayleigh-Jeans black body radiation, C_{window} is the power transmission coefficient through the vacuum window, and the relative visible area $V_{relat} = w^2/w_0^2$ (w is the Gaussian beam radius at the plasma surface).

plane stratified plasma slab which is inhomogeneous along the local density gradient. In this slab we solve Maxwell equations for wave propagation in a cold plasma by the finite element method with adaptive steps between nodes [5]. The power absorbed in the vicinity of the upper hybrid resonance due to weak collisions corresponds (if $\nu/\omega \rightarrow 0$) exactly to the power converted to the electron Bernstein waves. The reverse process is appropriate for ECE because we can assume reciprocity between emission and absorption.

Two processes here play a role: the direct EBW-X conversion as well as the process in which an obliquely incident EBW is first converted to an X mode which subsequently mode converts to an O-mode [6] at the plasma resonance.

We also use this slab model to determine the position of the UHR nearest to each spot and to obtain here the solution of the electrostatic dispersion relation of the electron Bernstein waves (EBW). This solution serves as an initial condition for the standard ray tracing [7] describing the propagation of EBW in 3D.

To determine the radiative temperature for Rayleigh-Jeans black body radiation we must solve, for each ray, the radiative transfer equation simultaneously with the

The integration is taken over the intersection of the waist and the projection of the vessel window rim onto the waist plane.

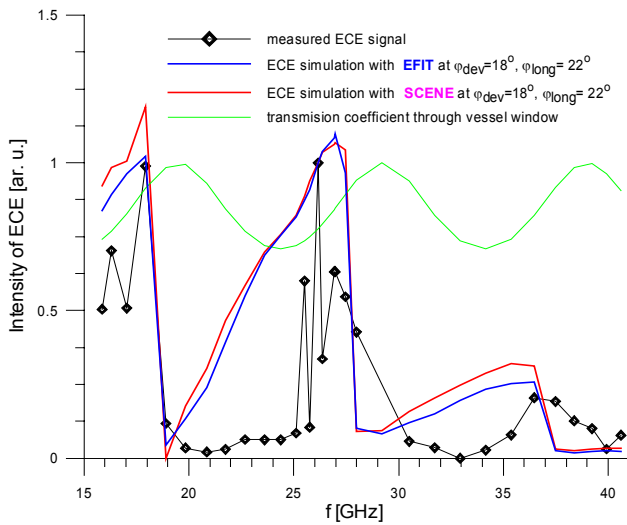


Fig. 4. Comparison of ECE simulations with EFIT and SCENE equilibria for ELMy H-mode #4958.

The best match between measured and simulated ECE can be found by variations of the antenna viewing angle. The accuracy of the antenna alignment is about 3° but also the diffraction of beam in rarefied plasma in SOL can be important. In Fig. 4 we compare the experimentally detected ECE for the discharge #7798 at $t=240\text{ms}$, when the density and temperature are measured by high resolution Thomson scattering, with the simulations for three different orientations of the antenna. In this paper we would like to investigate how the choice of a specific magnetic equilibrium can influence

ECE simulation and the fit with measured signal.

The most important changes can be anticipated in the shots where ELM-free H-mode is fully developed. We use the SCENE code for determining the magnetic configuration in

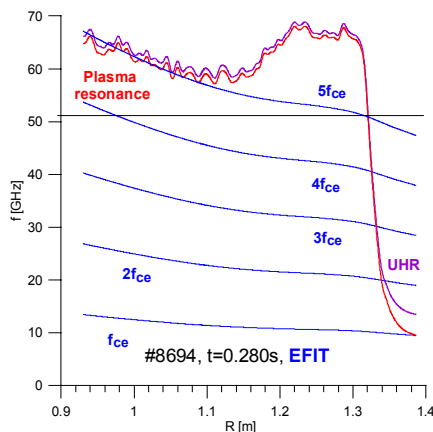


Fig. 5a. Radial profiles of the characteristic resonances for EFIT

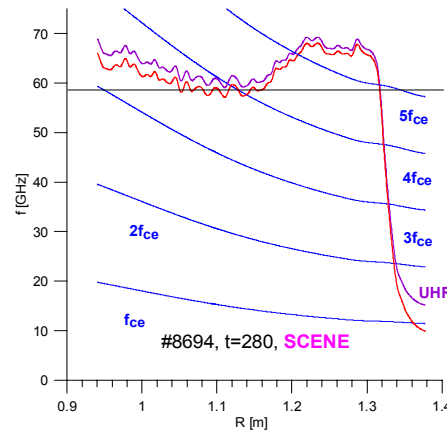


Fig. 5a. Radial profiles of the characteristic resonances for SCENE

our ECE simulations and compare results with ECE simulations using EFIT equilibrium reconstruction.

First we investigate the regular L-mode. ECE simulation fits well to the detected signal for such modes and, as we see from Fig. 3, SCENE and EFIT give similar results. For shot #7798, the conversion region for low frequency waves is situated in the highly turbulent plasma scrap-off layer. Under these conditions mode conversion is weak and non-robust. As a second example we investigated ELMy H-mode in the shot #4958. With appropriate beam angles the agreement with the experiment is good for both SCENE and EFIT equilibria but the suppressed ECE within the lower frequency part of the second and the third EC harmonic bands is not described well by any of simulation at any angle. This is typical for ELMy H-modes.

The situation is dramatically changed when we consider ELM-free H-modes. In Fig 5a,b., we depicted radial profiles of the characteristic resonances at beam spot ($\varphi_{\text{dev}} = \varphi_{\text{long}} = 12^\circ$). We see that the magnetic field estimated with SCENE is substantially stronger on the low field side of MAST. ECE simulation based on the EFIT (Fig. 6a) predicts wrong position of EC harmonic gaps namely the first two at 25 and 35GHz. Routine EFIT reconstruction does not account for the edge currents hence the effective magnetic field here is weaker. At the same time, the signals from five EC harmonic bands are clearly visible, which correspond to the internal field structure. If we use SCENE equilibrium (Fig. 6b), the position of the first two EC gaps fits well with ECE simulation, but a wrong number of EC bands is predicted.

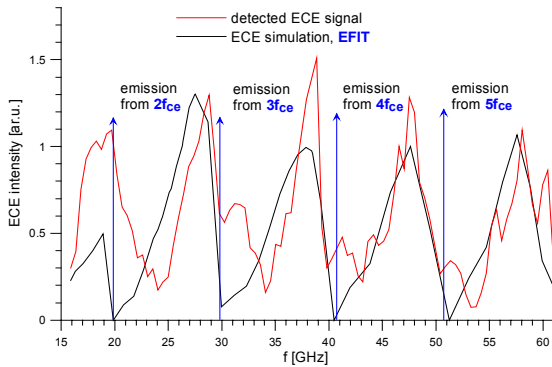


Fig. 6a. Detected ECE signal and the ECE simulation using EFIT equilibrium for ELM-free H-mode, #8694, $t=0.280$ s.

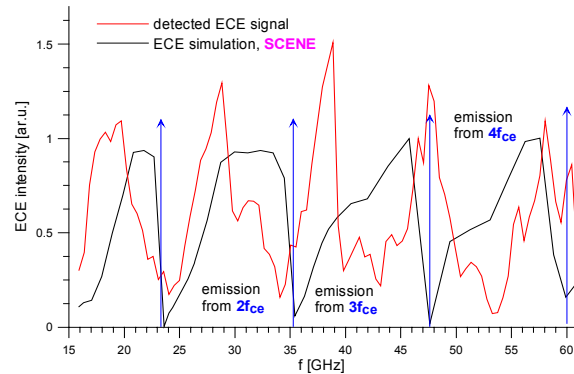


Fig. 6b. Detected ECE signal and the ECE simulation using SCENE equilibrium for ELM-free H-mode, #8694, $t=0.280$ s

Conclusions. We established good agreement for L-mode regimes between experimental ECE data and simulations based on magnetic equilibria obtained from EFIT and SCENE. For ELMy H-mode EFIT and SCENE give also similar results but ECE modeling fails to reproduce the suppressed emission level in the lower frequency part of each EC harmonic band. Situation is more complicated in ELM-free H-modes. Here SCENE describes well the situation at the plasma edge so ECE simulation predicts well the position of the first EC bands but the magnetic field in the bulk plasma is better predicted by EFIT. We are still in progress of developing the procedure, which would account for all necessary effects. We conclude that EBW emission must be used as an additional constraint in the reconstruction of an equilibrium, which would satisfy the experimental data.

Acknowledgement. Part of this work was funded jointly by the UK Engineering and Physical Sciences Research Council and by EURATOM.

References

- [1] Shevchenko V et al., *15th RF Power in Plasma*, Moran, 2003, edit. C. Forest, AIP **694**, 359.
- [2] Laqua H.P., et al., review, *15th RF Power in Plasma*, Moran, 2003, edit. C. Forest, AIP **694**, 15.
- [3] H.R. Wilson: SCENE, UKAEA FUS 271 (1974), Culham, Abingdon, UK
- [4] Preinhaelter J. e al, *15th RF Power in Plasma*, Moran, 2003, edit. C. Forest, AIP **694**, 388.
- [5] Urban J.: *Adaptive Finite Elements Method for the Solution of the Maxwell Equations in an Inhomogeneous Magnetized Plasma*, Diploma thesis, Czech Technical University in Prague, 2004
- [6] Preinhaelter J., Kopecky V., *J. Plasma Phys.* **10**, 1 (1973), part 1.
- [7] Pavlo P., Krlin L., Tluchor Z., *Nucl. Fusion* **31**, 711 (1991).